Direct measurement of the permeability of the meniscus bordering a free-standing smectic-*A* film

F. Caillier* and P. Oswald
Laboratoire de Physique de l'Ecole Normale Supérieure de Lyon, 46 Allée d'Italie, 69364 Lyon CEDEX 07, France
(Received 10 February 2004; revised manuscript received 22 April 2004; published 22 September 2004)

A smectic-*A* free-standing film is always connected by a meniscus to the frame on which it has been stretched. The meniscus acts as a dissipative reservoir and is characterized by its permeability. We propose a method to measure directly this quantity by equilibrating two menisci in correspondence with the same free-standing film. The permeability is shown to depend on the film thickness, in full agreement with previous indirect measurements obtained by analyzing the growth dynamics of dislocation loops. An improved model of the meniscus is proposed to interpret all the data.

DOI: 10.1103/PhysRevE.70.031704 PACS number(s): 61.30.Jf, 83.80.Xz

I. INTRODUCTION

In a smectic-*A* phase, the rodlike molecules are arranged in fluid layers with perpendicular orientation. In a free-standing film, the layers are always parallel to the free surfaces. In addition, the film is always attached to the frame on which it has been stretched via a meniscus of much larger volume than the film. For that reason, the meniscus acts as a reservoir of material [1] which fixes the pressure inside the film at equilibrium [2]. It turns out that the pressure inside the meniscus is always less than the atmospheric pressure due to its shape and the curvature of its interface with the air. As a result, the film, which is flat, is under compression. Nevertheless, it can easily withstand this stress without getting thinner because of the layer elasticity [2]. This is the reason why it is possible to prepare very stable films of varying thicknesses, from three to many thousands of layers. On the other hand, a film can get thinner if a pore (i.e., a dislocation loop) of radius larger than some critical radius nucleates inside the film. In that case, the loop radius r increases in time until the dislocation disappears into the meniscus. During this growth process, the film thickness decreases by a number of layers equal to the Burgers vector of the dislocation. In a recent work [3,4], it has been shown that the pore dynamics depends on both the film thickness and the permeability of the meniscus. In particular, it has been observed that the dislocation velocity tends to systematically decrease when its radius approaches that of the meniscus. This effect was explained within a theoretical model accounting for the finite permeability of the meniscus [5,6]. It allowed us to estimate this quantity by fitting the experimental curves $r(t)$ to a theoretical law. Nevertheless, this procedure is not precise as it strongly depends on quantities which are difficult to obtain, such as the line tension of the dislocation or the interaction energy between free surfaces, which enters into the expression for the force acting on the dislocation. Our goal in this article is to measure directly the permeability of the meniscus. This is essential to validate the model proposed for the meniscus in [5,6] and used in [3] to interpret the slowing down of the dislocation loops at large radius.

The article is organized into seven separate sections: In Sec. II, we recall the definition of the meniscus permeability. In Sec. III, we describe the experimental setup and the principle of the measurement, which consists of equilibrating two menisci of different sizes connected by a film of a known thickness. This is followed by Sec. IV, where we explain how the permeability can be found from the measurement of the time evolution of the size of the two menisci. Results are then given in Sec. V and compared to the previous measurements. Finally, all the data are reinterpreted in Sec. VI, in which we propose an improved version of the model of the meniscus given in Refs. [3,6], which takes into account the confinement of the dislocations. Conclusions are drawn in Sec. VII.

II. DEFINITION OF THE MENISCUS PERMEABILITY: THE $C(N)$ FUNCTION

In a previous work, we have shown that the meniscus does not behave as a perfect reservoir, but instead, as a very dissipative one [3–6] due to its lamellar structure. For that reason, a pressure difference must exist between the film and the meniscus when they exchange material. To a first approximation, we can suppose that this pressure difference is proportional to the flux of material:

$$P_N - P_m = \frac{C(N)}{\mu} v_m, \tag{1}$$

where P_N is the pressure inside the film (containing N layers), P_m the pressure inside the bulk of the meniscus, and v_m the velocity at the entrance of the meniscus (considered positive when the matter enters into the meniscus and negative, for matter leaving the meniscus). By definition, the meniscus permeability is the proportionality factor between the velocity v_m (assumed to be constant over the whole film thickness) and the pressure drop $P_N - P_m$. From the previous equation, this factor is expressed in the form $\mu_{men} = \mu / C(N)$ where μ is the usual dislocation mobility and $C(N)$ a dimensionless quantity which, for simplicity, we consider to only depend on the film thickness. This assumption is not obvious and will be discussed in Sec. VII. The fact that the mobility of the

*Author to whom correspondence should be addressed. Electronic address: francois.caillier@ens-lyon.fr

dislocations enters directly in the expression of the permeability comes from the fact that the dissipation in the meniscus is mainly due to the flow around the dislocations which pile up in the midplane of the meniscus in order to match its thickness variation.

We recall that the mobility μ is defined by the relation $v=\mu\sigma$, where v is the climb velocity of an edge dislocation under the action of a stress σ perpendicular to the layer. This quantity is well known in the smectic-*A* phase [7–9] and has been measured in 8CB both in bulk samples (from creep experiments [6,10]) and in smectic films [4,6,12].

The goal of this article is to measure directly the permeability of the meniscus or, equivalently, the $C(N)$ function as μ is known.

III. PRINCIPLE OF THE MEASUREMENT AND THE EXPERIMENTAL SETUP

A direct way to measure the permeability of a meniscus is to analyze the pressure equilibration between two menisci of different sizes when they are connected by a film of a given thickness. The feasibility of this experiment was shown earlier by Picano in his Ph.D. thesis [4], but no reliable results were obtained at this time.

The principle of the experiment is as follows.

(i) A film is first stretched with a spatula coated with the liquid crystal 8CB (4-*n*-octyl-4′-cyanobiphenyl from Merck Ltd) over a circular frame. In practice, the frame is made from a stainless steel foil of thickness $h_0=100$ μm in which a circular hole of radius $r_f=3$ mm has been drilled. The film thickness can be changed by stretching the film at different velocities. To simplify the process and make it more systematic, the spatula is fixed on a translation stage which is driven by a stepping motor. In that way, it is possible to choose the stretching velocity of the film. Experience shows that larger velocities lead to thinner films. This method allows us to prepare thick films, with N varying from 100 to many thousands. We note that more than a quarter of an hour is necessary to stretch a very thick film ($N>1000$). Once the film is stretched, it is allowed to equilibrate during half a day (sometimes more). During this time, the film thickness and the shape of the meniscus stabilize. The film thickness is then measured precisely by interferometry.

(ii) Once the film is prepared, it is pierced with a metallic needle of radius $r_n=0.3$ mm which has been previously coated with a small amount of 8CB. This precaution is necessary to avoid film rupture. It is worth noting than usually the film thickness does not change during this process (if it does, it can be measured again). We then wait many hours in order that the shape of the meniscus which forms around the needle stabilizes. The final configuration obtained this way is sketched in Fig. 1; it consists of a film connecting two circular menisci of different sizes. Note that because the film is thick, the two menisci match it tangentially [11,13]. As for the inner meniscus, it wets completely the needle as shown in the photograph of Fig. 2. The whole system is placed inside an oven which is regulated within ±0.05 °C. Finally, the film and two menisci are observed with a video camera connected to a computer via reflected light microscopy.

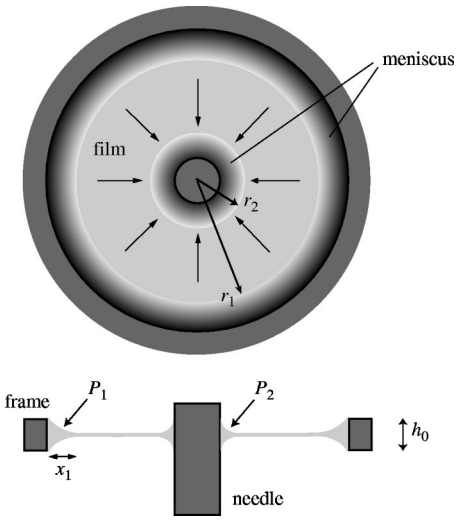

FIG. 1. Sketch of the experimental setup. A film is stretched between a needle and a circular frame. Because the pressures are different inside the two menisci, a flow occurs inside the film, which stops when the pressures are equilibrated. The arrows indicate the usual direction of the flow.

The principle of the measurement consists of measuring the flux of matter and the pressure inside each meniscus as a function of time. In the following section, we explain how these quantities are obtained in practice.

IV. DETERMINATION OF $C(N)$

With reference to Fig. 1, two quantities are easy to measure as a function of time with the aid of a microscope: the width x_1 of the outer meniscus (or, equivalently, its radius $r_1=r_f-x_1$) and the radius r_2 of the inner meniscus. In order to show how the measurement of these two quantities allow us to determine $C(N)$, let us first rewrite Eq. (1) for each meniscus. For the outer meniscus, we have

$$P_N - P_1 = -\frac{C(N)}{\mu} v_1, \tag{2}$$

where P_1 is the pressure inside the meniscus and v_1 the velocity at the entrance of the meniscus (which we take posi-

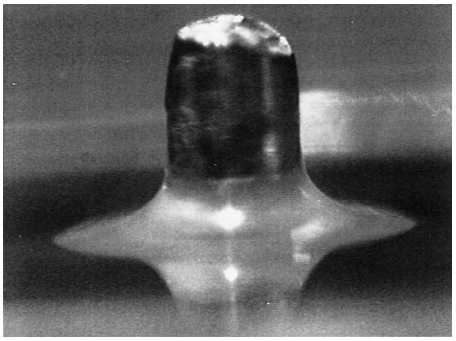

FIG. 2. Photograph taken with a macroscope of the needle surrounded by its meniscus. One clearly sees that the meniscus matches tangentially both the film and the surface of the needle.

tive, by convention). Note that we have introduced a minus sign in the right-hand side of this equation since the matter goes out of this meniscus which means that the material flows from the outer meniscus towards the inner one. For the inner meniscus surrounding the needle, we have

$$P_N - P_2 = \frac{C(N)}{\mu} v_2, \tag{3}$$

where P_2 is the pressure inside the inner meniscus. Because the mass is conserved, velocity v_2 must be equal to $(r_1/r_2)v_1$, which yields

$$P_N - P_2 = \frac{C(N)}{\mu}\frac{r_1}{r_2} v_1. \tag{4}$$

Substracting Eqs. (4) and (2), we obtain

$$v_1 = \frac{\mu}{C(N)}\frac{r_2}{r_1 + r_2}\Delta P, \tag{5}$$

where $\Delta P = P_1 - P_2$ is the pressure diffence between the two menisci.

It must be noted here that we have implicitly assumed that the pressure is constant inside the film. This is not exact in the presence of a two-dimensional radial flow [14] which leads necessarily to a pressure drop. The latter can be calculated from the Navier-Stokes equation, which gives [4]

$$\Delta P_N = P_{N1} - P_{N2} = 2\eta r_2 v_2 \left(\frac{1}{r_2^2} - \frac{1}{r_1^2}\right), \tag{6}$$

where P_{N1} (P_{N2}) is the pressure inside the film at $r = r_1$ (at $r = r_2$). This pressure drop is maximized by $2\eta v_2/r_2$. This quantity is always extremely small in comparison to the pressure differences at the entrance of the two menisci as $C \gg \eta\mu r_1^2/r_2 \sim 10^{-5}$ (in the following we shall see that in all experiments $C > 1$). So we can consider (within a very good approximation) that the pressure is constant inside the film (equal to P_N).

In practice, velocity v_1 is very small (less than 1 μm/h) and it cannot be measured directly (for instance, by following the motion of small particules scattered in the film). On the other hand, it can be related to the volume variation of one of the menisci, a quantity much easier to measure experimentally. Let V_2 (V_1) be the volume of the inner (outer) meniscus. According to the mass conservation law, $dV_2/dt = -dV_1/dt = 2\pi r_1 N d v_1$ (with d the layer thickness), which gives, after substitution into Eq. (5),

$$C(N) = 2\pi\mu N d \frac{r_1 r_2}{r_1 + r_2}\left(\frac{dV_2}{dt}\right)^{-1}\Delta P. \tag{7}$$

The following step consists of calculating the volume of the two menisci and their internal pressures as a function of the measured quantities x_1 and r_2. This can be done by solving numerically the Laplace law for each meniscus, which has been proved to apply to smectic meniscus in spite of their lamellar structure [2,6,11].

For the outer meniscus, of profile $\rho_1(z)$ in polar coordinates (see Fig. 3), this law reads

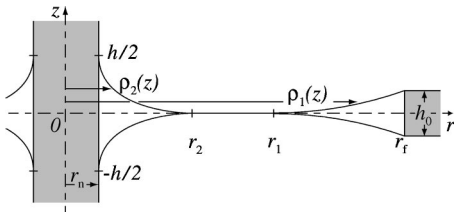

FIG. 3. Notations used for the numerical calculations.

$$\frac{\rho_1''}{(1+\rho_1'^2)^{3/2}} - \frac{1}{\rho_1\sqrt{1+\rho_1'^2}} = -\frac{\delta P_1}{\gamma}, \tag{8}$$

where $\delta P_1 = P_a - P_1 > 0$ is the pressure drop from the atmospheric pressure P_a and γ the surface tension [15]. Solving numerically this second-order differential equation with the boundary conditions

$$\rho_1(0) = r_1 = r_f - x_1,\ \rho_1'(0) = +\infty,\ \rho_1(h_0/2) = r_f \tag{9}$$

gives the pressure drop $\delta P_1(x_1)$ and the profile $\rho_1(z)$ from which the volume of the meniscus $V_1(x_1)$ can be calculated:

$$V_1(x_1) = 2\int_0^{h_0/2} \pi[r_f^2 - \rho_1^2(z,x_1)]dz. \tag{10}$$

The functions $\delta P_1(x_1)$ and $V_1(x_1)$ are plotted in Fig. 4.

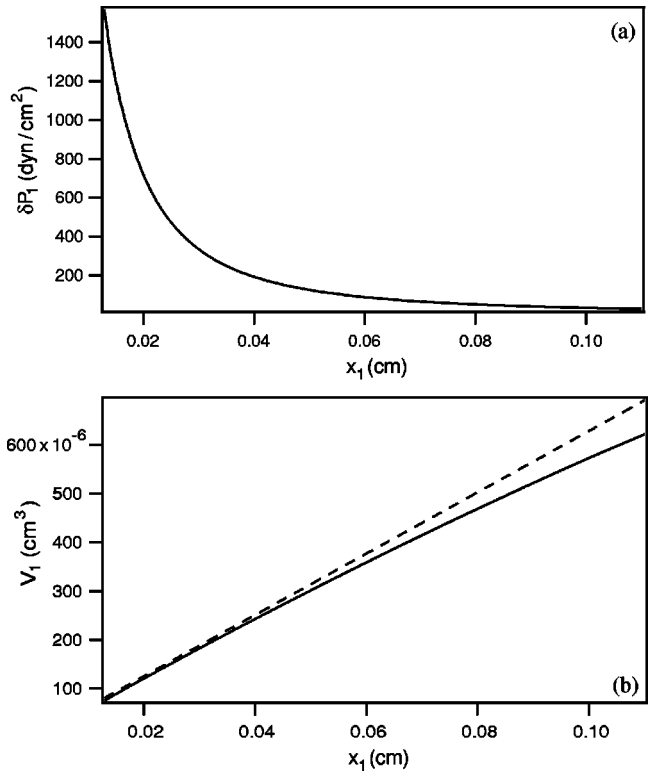

FIG. 4. Pressure drop δP_1 (a) and volume V_1 (b) numerically calculated from Eqs. (8)–(10) as a function of the width x_1 of the outer meniscus. The dotted line has been calculated by using the approximate formula $V_1 = (2/3)\pi r_f h_0 x_1$.

It must be emphasized that in this calculation, we have assumed that the height of the meniscus at $r=r_f$ is exactly equal to the frame thickness h_0. This boundary condition can be checked visually by observing the frame under grazing incidence, which shows that there is no visible matter in excess at the surface of the frame. Another much more convincing way to check this crucial point consists of measuring the radius of curvature of the meniscus at the matching point with the film (at $r=r_1$). This can be done very accurately by measuring via reflected light microscopy the profile of the meniscus [2]. This measurement and knowledge of the width x_1 of the meniscus allow us to calculate its height h at $r=r_f$. The value found in this way is equal to the frame thickness within ± 2 μm, confirming our assumption that $h(r=r_f)=h_0$.

The same numerical procedure can be applied for the inner meniscus. It yields, by denoting $\rho_2(z)$ the surface profile (Fig. 3) and $\delta P_2 = P_a - P_2 > 0$ the pressure drop,

$$\frac{\rho_2''}{(1+\rho_2'^2)^{3/2}} - \frac{1}{\rho_2\sqrt{1+\rho_2'^2}} = \frac{\delta P_2}{\gamma}, \tag{11}$$

with the boundary counditions

$$\rho_2(0) = r_2,\ \rho_2'(0) = -\infty,\ \rho_2'(h/2) = 0,\ \rho_2(h/2) = r_n. \tag{12}$$

Solving this equation gives the pressure drop $\delta P_2(r_2)$, the height h of the meniscus on the needle, and its complete profile $\rho_2(z)$ from which we can calculate the volume $V_2(r_2)$ using

$$V_2(r_2) = 2\int_0^{h/2} \pi[\rho_2^2(z,r_2) - r_n^2]dz. \tag{13}$$

The functions $\delta P_2(x_2)$ and $V_2(x_2)$ are plotted in Fig. 5.

Note that we have neglected the effect of gravity as the heights of the two menisci (h_0 and h) are small experimentally in comparison to the capillary gravitational length $\sqrt{\gamma/\rho g} \approx 2$ mm.

Note also that in Eqs. (8) and (11), the two first terms on their left-hand side correspond, respectively, to the interface curvature in the radial plane $(1/R_1)$ and to the curvature interface in the orthogonal plane containing the normal to the interface $(1/R_2)$. For the outer meniscus $(1/R_1 \gg 1/R_2)$ and the second term could be neglected. A consequence is that V_1 increases almost linearly as a function of x_1 as shown in Fig. 4(b). This curve is indeed fairly close to what we calculate to the first order in x_1/R_1 by neglecting the radius of curvature R_2. Within this approximation, the meniscus has a circular profile and its volume may be expressed in the form $V_1 \approx (2/3)\pi r_f h_0 x_1$ [dotted line in Fig. 4(b)]. In contrast, $1/R_1 \sim 1/R_2$ for the inner meniscus due to the small radius of the needle and the two terms must be kept, imposing a numerical solution to resolve the equation.

We can now deduce $C(N)$ from the curves $x_1(t)$ and $r_2(t)$ measured experimentally. Indeed, for each data set $[x_1(t), r_2(t)]$ we can deduce $V_1(t)$ and $V_2(t)$ as well as $\delta P_1(t)$ and $\delta P_2(t)$ from the graphs of Figs. 4 and 5. This then allows us to calculate dV_1/dt (in principle equal to $-dV_2/dt$ if the total volume is conserved, as we have assumed from the beginning) and the pressure difference $\Delta P = P_1 - P_2 = \delta P_2 - \delta P_1$. Finally $C(N)$ is obtained from Eq. (7).

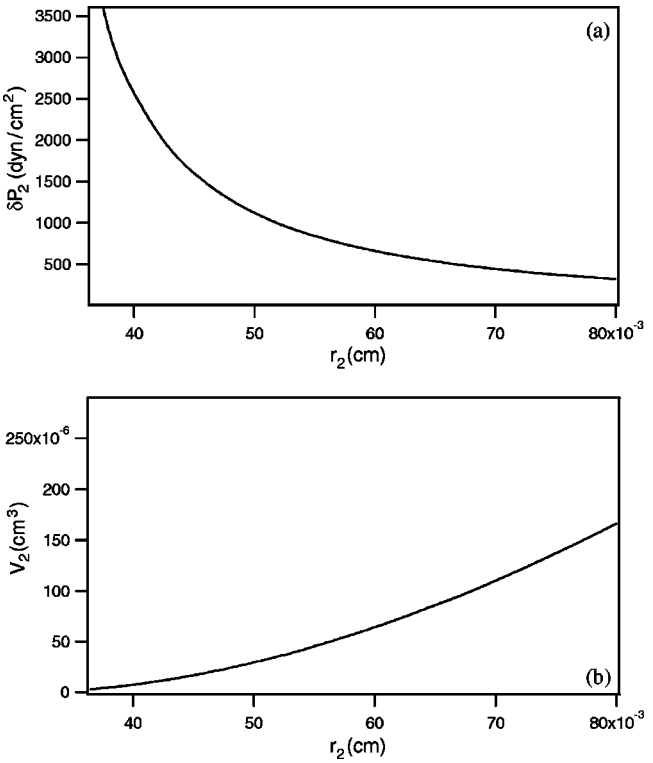

FIG. 5. Pressure drop δP_2 (a) and volume V_2 (b) numerically calculated from Eqs. (11)–(13) as a function of the radius r_2 of the inner meniscus.

V. EXPERIMENTAL RESULTS

An example of a complete set of data obtained with a film of thickness $N=633$ is shown in Fig. 6. The first graph shows absolute measurements of x_1 and r_2 as a function of time. These values are obtained by displacing the system (film + frame + needle) under the microscope with a precision translation stage. The edges of the menisci at their matching points with the film are located by analyzing the interference fringes which form inside the menisci in reflected light. The accuracy of these measurements is of the order of ± 3 μm. The second graph reports the pressure drops measured in both menisci as a function of time. As expected, the pressures are different at the beginning and tend to equilibrate in time, and are essentially the same after two weeks. In the third graph, the volumes of the meniscus are reported as a function of time. As expected, the inner meniscus empties into the outer meniscus. The total volume of the two menisci is also reported in this graph—it remains constant, which means there is no leak of material out of the system. This point was important to check as one could fear that the liquid crystal flows out by capillarity at the surface of the frame or the needle. These curves also show that the relaxation takes place in two steps: it is fast during the first day, as long as the pressure difference between the two menisci is larger than about 100 dyn/cm^2; on the other hand, it slows down enor-

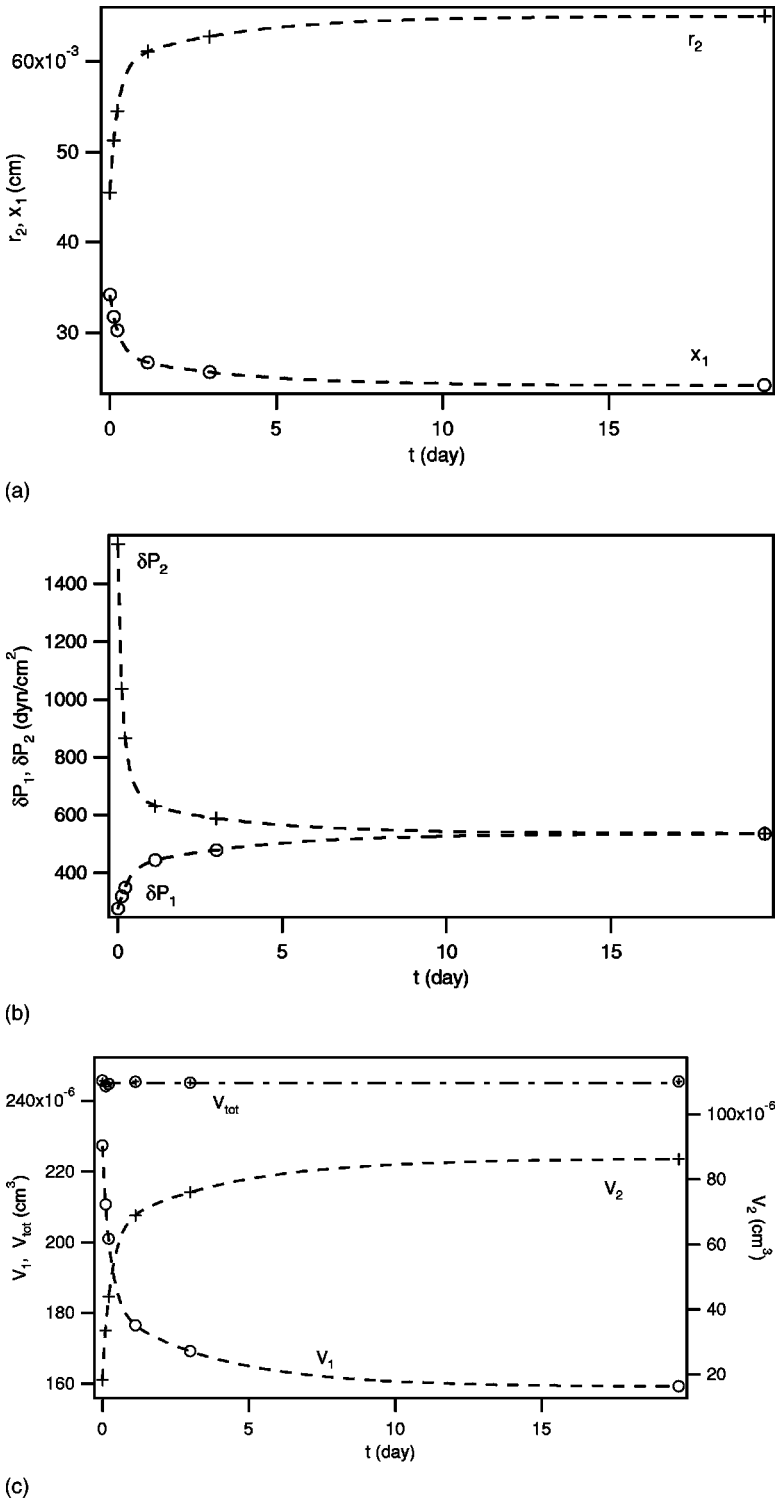

FIG. 6. (a) Radius r_2 and width x_1 measured experimentally as a function of time. (b) Pressure drops δP_1 and δP_2 obtained from the graphs of Figs. (3a) and 4(a). (c) Volumes V_1 and V_2 obtained from the graphs of Figs. (3b) and 4(b). The film thickness is $N=633$. These graphs show that the pressures inside the two meniscus need two weeks to equilibrate. The total volume $V_{tot}=V_1+V_2$ is also plotted in (c). It is constant, which means that the material is conserved. Lines are just a guide for the eye.

mously after 1 day, as 2 weeks are then necessary to reach a complete equilibrium. This slowing down was systematically observed in all of our experiments, whatever the film thickness, as long as the pressure difference between the two menisci was inferior to typically 100 dyn/cm^2.

From these measurements, it is possible (in principle) to extract the value of C by using Eq. (7). Nevertheless, this requires us to calculate dV_2/dt from the experimental curve $V_2(t)$. Doing that from the curve shown in Fig. 6 is impossible due to a lack of precision in the data: indeed, if the absolute measurements of r_2 and x_1 are sufficiently precise to check the conservation of the total volume during the whole experiment, they are not precise enough to determine dV_2/dt.

To obtain a more precise value of dV_2/dt between each absolute determinations of r_2 and x_1, we measured very accurately the relative variation of radius $r_2(t)$ [or $x_1(t)$] over 2–3 h. To do that, we digitized and recorded at regular time intervals the images in the microscope of the edge of the

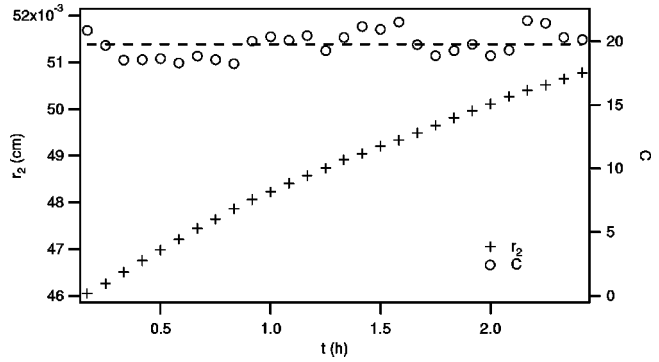

FIG. 7. Constant C measured during the period of fast equilibration (between the first two points in Fig. 5) ($N=633$). The radius r_2 is measured very precisely by using a high-magnification objective. In this regime C is constant.

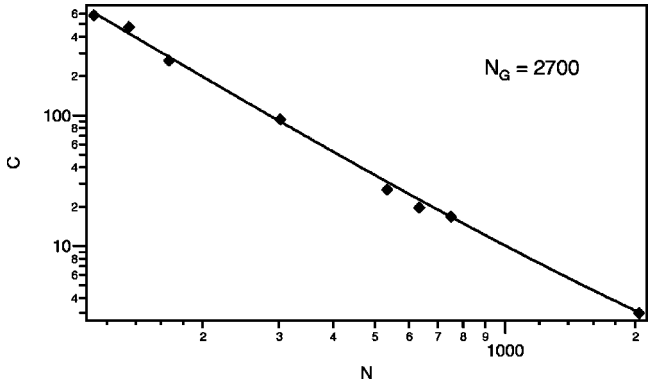

FIG. 8. Constant C as a function of N (log-log representation). All measurements have been performed during the period of fast relaxation, when the pressure difference between the two menisci is typically more than 200 dyn/cm^2. The line is the best fit to the power law $(N_G/N)^2$.

meniscus (note that during this sequence the film is fixed with respect to the microscope). An objective of large magnification ($40\times$) was used to increase the precision, as well as a high-resolution camera (Hamamatsu C4742-95). Each image is then analyzed in order to detect the position of the edge of the meniscus. It must be emphasized that because the film and meniscus match tangentially, the edge of the meniscus is impossible to localize visually. For that reason, we plotted the intensity profile of the reflected light in the direction perpendicular to the edge. Because of the thickness variation of the meniscus, this profile oscillates and shows interference fringes [2]. It is then possible to detect very accurately (within ± 0.5 μm) the position of the first interference fringe, which we suppose to be at a constant distance of the edge of the meniscus. This is not exactly rigorous because the radius of curvature of the meniscus changes slightly during the whole sequence, but it is possible to check that the error made by measuring dx_2/dt in this way is less than 1%. A sequence of 2 h realized during the stage of fast relaxation described before (see Fig. 6) is shown in Fig. 7. The time interval between two measurements is 5 mn. During these 2 h, the edge of the meniscus (more exactly the position of the first interference fringe) moved over a distance of the order of 50 μm. These measurements allowed us to determine accurately dV_2/dt. Because r_1 was not measurable simultaneously, it was necessary to calculate it from the graph in Fig. 4(b). This was possible because we know that the total volume remains constant; thus measuring r_2 gives V_2 from which $V_1=V_{tot}-V_2$ and, then, r_1 can be deduced. In this way, it was possible to measure C as a function of time. Figure 7 shows that C is constant, within experimental errors, over the whole duration of the recording. Experimental results show that the value of C found this way is constant as long as the measurement is done during the fast relaxation stage. To the contrary, C starts to strongly increase if the measurement is performed during the late-stage relaxation process—i.e., typically, when the pressure difference between the two menisci is less than 100 dyn/cm^2. This point is not very well understood and will be discussed in Sec. VII.

This experiment was repeated for films of different thicknesses and menisci of different sizes. In all cases, C was measured during the early stage of the relaxation, after the shapes of the menisci were stabilized. We checked that for each film of a given thickness, C is constant (i.e., independent of the size of the meniscus) provided that the pressure difference between the two menisci is large enough. In contrast, C strongly depends on the film thickness N, as can be seen in Fig. 8. This graph shows that in the range of thicknesses we have studied, C varies like

$$C(N) = \left(\frac{N_G}{N}\right)^2 \quad (110 < N < 2000), \tag{14}$$

with $N_G \approx 2700$ layers, whatever the size of the meniscus. This expression shows that C quickly increases as the film thickness decreases. This is the reason why we were not able to do measurements in thin films (less than 100 layers). Indeed, the meniscus relaxation time becomes so large that it becomes impossible to measure it. To give an example, if 2 weeks are necessary to equilibrate two menisci with a film of about 600 layers, more than 1 year (72 weeks) is required according to Eq. (14) to do the same with a film of 100 layers. As a consequence, this method of measurement is only applicable to relatively thick films. It turns out that it was exactly the contrary in the previous work on dislocation dynamics, where the finite permeability of the meniscus had only a visible effect in thin films ($N<100$, typically). For this reason, these two experiments are complementary. In the following section, we compare the results obtained by these two methods.

VI. COMPARISON WITH THE PREVIOUS MEASUREMENTS AND OUR MODEL OF THE MENISCUS

In Fig. 9, we put together in the same graph all the results obtained by the two methods. The crosses correspond to the present measurements, while the circles have been obtained from the experiments on the pore dynamics [3] consisting of measuring their radius versus time in films of different thicknesses. This figure shows that the two methods give values of the same order of magnitude in the narrow range of thicknesses where they are both applicable (between 100 and 150

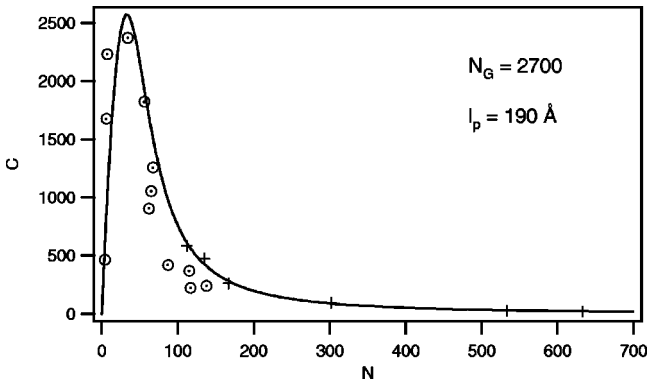

FIG. 9. Contant C as a function of N: the whole set of the experimental results. Crosses correspond to the experiment on the equilibration of the two meniscus; circles have been observed from the pore dynamics experiment (from Ref. [3]). The solid line is the best fit to Eq. (18).

layers, typically). Nevertheless, we emphasize that in this range of thicknesses, both methods are very imprecise, as the meniscus equilibration time starts to be very long, while the slowing down of the pores (which is due to finite permeability of the meniscus) becomes negligible and very difficult to detect. This is due to the fact that the thicker the film, the smaller is the dissipation due to the flow in the meniscus induced by the growth of the pore. This is easily understandable as, according to the mass conservation law, the velocity v_m at the entrance of the meniscus is equal to vr/Nr_1 where v is the pore growth velocity and r its radius. As a consequence the dissipation in the meniscus is maximal when $r=r_1$ and equals [using Eq. (14)] $\Phi=[(C(N)/\mu)v_m]\times[2\pi r_1 N d v_m]=2\pi r_1 d N_G^2 v^2/(\mu N^3)$. The $1/N^3$ decrease of Φ explains why the slowing down of the loop becomes completely negligible in thick films (more than 150 layers).

In order to interpret the whole curve and the dissipative behavior of the menisci due to their lamellar structure, we have previously proposed a model of meniscus in Ref. [3]. This model is summarized in Fig. 10 and consists of considering the flow around the dislocations which lie in the middle plane of the meniscus. The fact that the dislocations are localized in the bulk of the meniscus is due to their repulsion

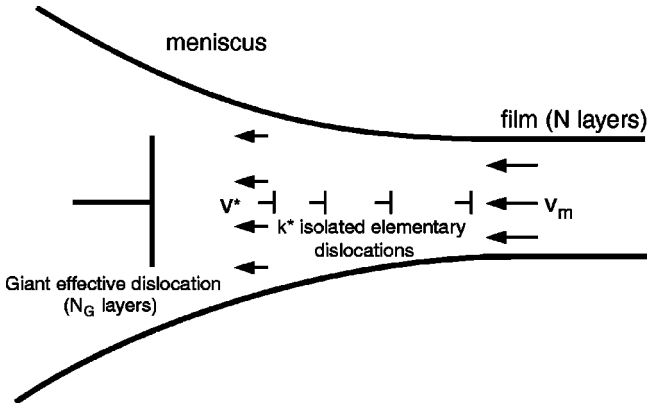

FIG. 10. Model of the meniscus used to calculate its permeability (from Ref. [3]).

from the free surfaces as shown previously both theoretically [6,16–18] and experimentally [6,18,19]. In the model, the dislocations are separated in two groups: (i) k^* dislocations which can be considered as independent from each other from a hydrodynamic point of view and (ii) all the other dislocations which are situated in the part of the meniscus that is well oriented [6,11].

In this model, all the dislocations of the second group are treated like a giant dislocation of Burgers vector $N_G d$. The reason for this is that they are so close to each other that they block the flow in the middle plane of the meniscus. A giant dislocation mimics this situation from a pure hydrodynamical point of view. By further assuming that all the dislocations have the same mobility, this model leads to the following formula [3,6]:

$$C(N) = \frac{k^*}{k^* + N} + N_G \frac{N}{(N + k^* - 1)^2}, \tag{15}$$

where k^* is an integer number given by

$$k^* (N + k^*)^4 = \frac{4 l_p^2 R}{d^3}. \tag{16}$$

In this equation, R is the radius of curvature of the free surface of the meniscus and $l_p = \sqrt{\eta \lambda_p}$ is the permeation length (with λ_p the permeation coefficient and η the shear viscosity parallel to the layers). This length is usually expected to be of the order of a molecular length [6].

Solving numerically Eq. (15) shows that k^* is equal to zero in thick films of typically more than 100 layers and depends little on R in thinner ones ($k^* \propto R^{1/5}$ in very thin films). As a consequence, $C(N)$ is nearly independent of the meniscus size, in agreement with experiments. This model also predicts that the curve $C(N)$ has a maximum, as observed experimentally. On the other hand, it leads to a $1/N$ variation of $C(N)$ at large N, a result that disagrees with our experimental data, which displays a $1/N^2$ dependence in the range $150 < N < 2000$ [see Eq. (14) and Fig. 8].

This point can be easily corrected by taking into account the fact that the giant dislocation of Burgers vector $N_G d$ is confined between the two free surfaces of the meniscus. More precisely, the number of layers in the meniscus equals $N + k^*$ upstream from the dislocation and $N_G + N + k^*$ downstream from the dislocation. As a consequence, we can consider the giant dislocation to move in a film of thickness $N_G + N + k^*$. In Ref. [6] (p. 104), it has been shown that the mobility of a dislocation of Burgers vector b in a free film of thickness H is given by the formula

$$\mu(H) = \mu \frac{H - b}{H}, \tag{17}$$

where μ is the mobility in a bulk sample.

Applying this formula to the giant dislocation in the meniscus gives its real mobility:

$$\mu_G = \mu \frac{N + k^*}{N_G + N + k^*}. \tag{18}$$

In principle, the same reasoning must be applied to the other elementary dislocations situated between the entrance of the meniscus and the giant dislocation. For instance, the mobility of the *i*th dislocation reads, according to Eq. (17),

$$\mu_i = \mu \frac{N+i-1}{N+i} \quad (1 < i < k^*). \tag{19}$$

In practice $N+i$ is always much larger than 1, so the confinement effect can be neglected for all of these dislocations ($\mu_i \approx \mu$).

Finally, Eq. (16) remains unchanged and Eq. (15) becomes, after taking into account the confinement effect of the giant dislocation,

$$C(N) = \frac{k^*}{k^* + N} + N_G \frac{N}{(N+k^*-1)^2} \frac{N_G + N + k^*}{N + k^*}. \tag{20}$$

In this equation the first term in the right-hand side remains unchanged as it corresponds to the dissipation due to the k^* dislocations for which the mobility is constant and equal to μ.

This expression has been used to fit our experimental data. The theoretical curve is shown in Fig. 9 (solid line). We see that it passes very well through the experimental points obtained from the method of equilibration of the menisci (crosses in the graph). In addition, it can be verified that Eq. (20) simplifies in this range of thicknesses and reads as Eq. (14) which was determined experimentally. The theoretical curve also passes through a maximum and fits fairly well the previous data obtained by analyzing the pore dynamics [3]. On the other hand, the values of N_G and l_p found by fitting the experimental data to expression (20), namely,

$$N_G \approx 2700 \text{ and } l_p \approx 190 \text{ Å}, \tag{21}$$

are significantly different from those obtained by fitting the data to Eq. (15): $N_G = 58\,000$ and $l_p = 15$ Å (values given in Ref. [3]).

It turns out that these new values are much more satisfactory. Indeed, $N_G = 2700$ correspond to a giant dislocation of Burgers vector $b = 7$ μm (instead of $b = 170$ μm). This result suggests that dissipation takes place essentially close to the edge of the meniscus in a typical band width of $W \sim (RN_G d)^{1/2}$ where R is the radius of curvature of the meniscus. Taking as a typical value $R = 1$ mm, it gives $W \sim 100$ μm. As can be seen in the photograph of Fig. 11, this value coincides with the width of the zone of the meniscus which is well oriented and does not contain any focal conic defects. Beyond this limit, the elementary dislocations group together (this result was demonstrated in Ref. [11]) and destabilize to form oily streaks which are composed of focal conics [20].

As for the value of l_p, it is found to be 10 times larger than before (about $6d$ instead of $0.5d$). This estimate suggests that the permeation is fairly easy in 8CB. This is quite possible and, even, agrees with the experimental fact that the mobility of edge dislocations is independent of their velocity. Indeed, it has been shown theoretically [9] that the dislocation mobility is constant and given by the classical formula $\mu = \sqrt{\lambda_p / \eta}$ only in the limit $l_p \gg \lambda$, where λ is the smectic penetration length (found of the order of 10 Å in 8CB; see [6]). In addition, the relation $l_p = \eta\mu$ is now satisfied as we know from previous measurements that $\eta \simeq 5$ P [6] and $\mu \simeq 4 \times 10^{-7}$ cm/P [6,11], which gives $\eta\mu \simeq 200$ Å in very good agreement with our estimate of l_p.

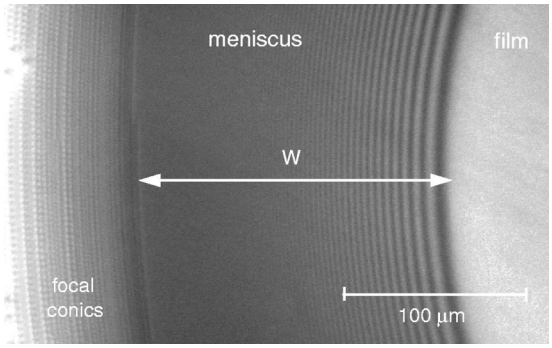

FIG. 11. Photograph of the meniscus taken from the microscope. Three regions are clearly visible: the film, on the right; a band, in the middle, in which there is no visible defects; the bulk meniscus, on the left, in which focal conics are clearly visible. Note that in the central region, the only thing we see are the interference fringes which can be used to detect the meniscus profile—in this region the layers are well oriented and form a grain boundary in the midplane, only composed by elementary edge dislocations (from Ref. [11]).

VII. CONCLUDING REMARKS

In conclusion, we have shown that equilibrating two menisci of different sizes allows us to determinate their permeability. In agreement with previous measurements on pore dynamics, we find that the permeability of a meniscus strongly depends on the film thickness, and very little on its size. This result is compatible with the usual structure of the menisci, which are always formed by two well-characterized regions: one, bordering the planar film, in which layers are perfectly organized and form an array of elementary edge dislocations located in the middle plane [11], and a second one, starting from the place (clearly visible in the microscope; see Fig. 2) where the dislocations group together by forming giant dislocations, which minimizes their energy [11]. As shown theoretically and experimentally in Ref. [20], giant dislocations are unstable with respect to the formation of focal conic domains [6,21], so that the smectic layers are rapidly disoriented in this region (see again the photograph in Fig. 11).

In our model, we have implicitly assumed that the dissipation only takes place in the first region. As a consequence, we have completely neglected the dissipation inside the disorganized region of the deformable meniscus. In other words, we have assumed that the second region, which represents the biggest part of the meniscus, acts as a perfect reservoir. Experimentally, this assumption is clearly valid when the flux of matter is large enough—i.e., as long as a significant pressure difference exists between the two menisci (in practice, typically more than 100 dyn/cm^2). In this limit, experimental results are reproducible. This is due to

the fact that the structure of the well-organized region of the meniscus bordering the film is robust and does not depend on the film preparation as can be checked experimentally.

On the other hand, our observations suggest that the dissipation inside the bulk meniscus becomes important, and even dominates the relaxation at the end of the process, when the deformation rate of the meniscus tends to zero. This could easily be explained by considering that the bulk meniscus behaves like a shear-thinning viscous fluid with a yield stress below which its effective viscosity would abruptly increase. This explanation is supported by previous measurements of the shear viscosity of the smectic phase in the presence of focal conics, which clearly showed a Bingham-type behavior [6,22].

ACKNOWLEDGMENTS

We thank J.-C. Géminard and V. Bergeron for fruitful discussions.

[1] P. Pieranski, L. Beliard, J.Ph. Tournellec, X. Leoncini, C. Furtlehner, H. Dumoulin, E. Riou, B. Jouvin, F.P. Fénerol, Ph. Palaric, J. Heuving, B. Cartier, and I. Kraus, Physica A **194**, 364 (1993).
[2] J.C. Géminard, R. Holyst, and P. Oswald, Phys. Rev. Lett. **78**, 1924 (1997).
[3] P. Oswald, F. Picano, and F. Caillier, Phys. Rev. E **68**, 061701 (2003).
[4] F. Picano, Ph.D thesis, Ecole Normale Supérieure de Lyon, 2001.
[5] P. Oswald, P. Pieranski, F. Picano, and R. Holyst, Phys. Rev. E **88**, 015503 (2002).
[6] P. Oswald and P. Pieranski, *Les Cristaux Liquides: Concepts et Propriétés Physiques Illustrés par des Expériences* (GB Science Publishers-Contemporary Publishing International, Paris, 2002), Vol. 2.
[7] M. Kléman and C.E. Williams, J. Phys. (France) Lett. **35**, L49 (1974).
[8] Orsay Group on Liquid Crystals, J. Phys. (Paris), Colloq. **36**, C1-305 (1975).
[9] E. Dubois-Violette, E. Guazzelli, and J. Prost, Philos. Mag. A **44**, 727 (1983).
[10] P. Oswald, C. R. Seances Acad. Sci., Ser. 2 **296**, 1385 (1983);P. Oswald and M. Kléman, J. Phys. (France) Lett. **45**, L–319 (1984).
[11] F. Picano, R. Holyst, and P. Oswald, Phys. Rev. E **62**, 3747 (2000).
[12] F. Picano, P. Oswald, and E. Kats, Phys. Rev. E **63**, 021705 (2001).
[13] A. Poniewierski, P. Oswald, and R. Holyst, Langmuir **18**, 1511 (2002).
[14] The situation would be completely different with a soap film because a Poiseuille flow develops within the film thickness when it gets thinner. See, for instance, A.A. Sonin and D. Langevin, Europhys. Lett. **22**, 271 (1993).
[15] R. Jaquet and F. Schneider, Phys. Rev. E **67**, 021707 (2003).
[16] L. Lejcek and P. Oswald, J. Phys. II **1**, 931 (1991).
[17] M.S. Turner, M. Maaloum, D. Ausséré, J.-F. Joanny, and M. Kunz, J. Phys. II **4**, 689 (1994).
[18] R. Holyst and P. Oswald, Int. J. Mod. Phys. B **9**, 1515 (1995).
[19] M. Maaloum, D. Ausserré, D. Chatenay, G. Coulon, and Y. Gallot, Phys. Rev. Lett. **68**, 1575 (1992).
[20] P. Boltenhagen, O. Lavrentovich, and M. Kléman, J. Phys. II **1**, 1233 (1991).
[21] Y. Bouligand, J. Phys. (Paris) **33**, 525 (1972).
[22] R.G. Horn and M. Kléman, Ann. Phys. **3**, 229 (1978).